ACS Pharmacology & Translational Science

pubs.acs.org/ptsci

Article

In-Depth Characterization for Methionine Oxidization in Complementary Domain Region by Hydrophobic Interaction Chromatography

Liu Tang,[‡] Huiliang Geng,[‡] Lei Zhang,* Xinyi Wang, Mengdan Fei, Boyuan Yang, Haijie Sun, and Zhongli Zhang*

Cite This: https://doi.org/10.1021/acsptsci.4c00296

Read Online

ACCESS | Metrics & More | Article Recommendations | Supporting Information

ABSTRACT: The oxidation of the complementarity-determining region (CDR) in monoclonal antibodies (mAbs) is a critical quality attribute that can affect the clinical efficacy and safety of recombinant mAb therapeutics. In this study, a robust hydrophobic interaction chromatography (HIC) method was developed to quantify and characterize CDR oxidation variants in mAb-A by using a Proteomix Butyl-NP5 column. The HIC analysis revealed oxidation variants that eluted earlier than the main species with weaker hydrophobicity. It was found that Met_{105} in the CDR was more susceptible to oxidation. Additionally, it was noted that the oxidation of Met_{105} on a single heavy chain resulted in elution at a distinct position compared to the oxidation on two heavy chains. This observation led to the fractionation and enrichment of the oxidized variants for further evaluation of their biofunction. The study also demonstrated that the oxidation of Met_{105} did not impact the antigen-binding capacity but significantly reduced the PD-1/PD-L1 blockade activity of mAb-A. The HIC method, which was employed to quantify CDR oxidation, underwent validation and was subsequently utilized for stability studies as well as for assessing the similarity between mAb-A and its reference product.

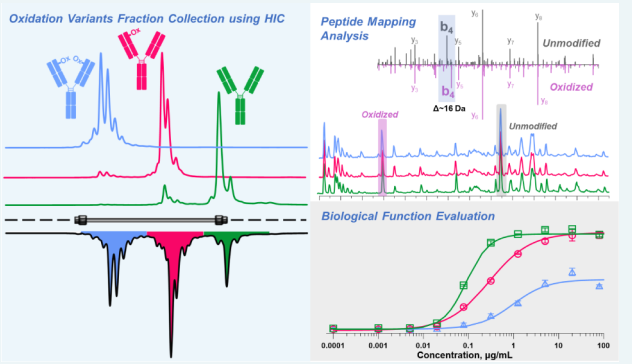

KEYWORDS: *monoclonal antibodies, oxidation, hydrophobic interaction chromatography, peptide mapping, IdeS digestion*

Oxidation is a common degradation pathway for monoclonal antibodies, and it can occur during manufacturing or storage processes due to various factors, such as dissolved oxygen, metal ions, hydrogen peroxide, as well as UV light.[1,2] Oxidation can lead to changes in conformation stability and impact the safety and efficacy of antibodies.[3] The most common oxidation residues are methionine (Met) and tryptophan (Trp), though oxidations of other residues such as cysteine (Cys), histidine (His), and lysine (Lys) have also been observed.[4,5]

The position of the oxidation sites is critical for the structural and functional properties of protein. The oxidation of Met or Trp residues in the fragment crystallizable (Fc) region can change secondary and tertiary structures, impair Fc-mediated activity,[6,7] and reduce the half-life of antibodies.[8] For example, Met_{252} oxidation has been reported to affect the binding activity to the neonatal Fc receptor (FcRn) and, in turn, the pharmacokinetics (PK) of product.[9] Additionally, Trp_{47} oxidation in the complementarity-determining region (CDR) can lead to a progressive loss of potency in antigen-binding capabilities.[10] Oxidation can also reduce physical stability[11−13] and increase immunogenicity of antibodies.[14,15]

Given that oxidation can occur at various stages of antibody development, it is crucial to establish a sensitive and reliable method for monitoring oxidative variants. Several physico-chemical methods are available for determining oxidative variants, including size exclusion chromatography (SEC),[16,17] cation exchange chromatography (CEX),[18−20] liquid chromatography−mass spectrometry (LC-MS),[21−23] reversed-phase high-performance liquid chromatography (RP-HPLC), and hydrophobic interaction chromatography (HIC). RP-HPLC is commonly used for separating oxidized variants,[24,25] but it is a denaturing method and cannot provide native oxidation variants for functional studies.

As a complementary technique to RP-HPLC, HIC offers the ability to separate oxidation variants based on their differing hydrophobicity.[26] One advantage of the HIC method is its ability to perform separations under natural conditions, such as physiological pH, mild column temperature, and low

Received: May 21, 2024
Revised: June 29, 2024
Accepted: July 5, 2024

concentrations or even without the need for organic solvents. This allows proteins to maintain their noncovalent interactions and higher-order structures.[27−32] Additionally, HIC is widely utilized in the separation of other post-translational modification variants,[33,34] as well as in the evaluation of drug−antibody ratios and drug loading distributions in antibody−drug conjugates,[35,36] and the analysis of heterodimerization in bispecific antibodies.[37,38] Currently, HIC has emerged as the most crucial chromatographic method for analyzing oxidative variants. Previous studies have demonstrated that HIC can effectively determine tryptophan oxidation in the CDR[10] and methionine oxidation in the Fc region.[39] However, there have been no reports on the application of HIC for separating methionine oxidation in the CDR region.

Keytruda, a highly successful drug developed by Merck and approved by the Food and Drug Administration in 2014, is a programmed death 1 (PD-1) inhibitor widely used for treating various cancers such as triple-negative breast cancer (TNBC), melanoma, non-small-cell lung cancer (NSCLC), and head and neck squamous cell cancer (HNSCC). In this study, we established a validated HIC method to quantitatively analyze methionine oxidation in the CDR of mAb-A, a biosimilar to pembrolizumab developed by Shanghai Henlius Biopharmaceutical Co., Ltd. The results were further confirmed through a peptide mapping analysis. Additionally, HIC analysis revealed similar degradation pathways and trends for mAb-A and Keytruda under forced oxidation conditions. By collecting and characterizing HIC components, we were able to confirm the oxidation sites and evaluate their impact on functionality.

EXPERIMENTAL SECTION

Reagents. 2-(*N*-Morpholino) ethanesulfonic acid (MES), Tris-base, iodoacetamide (IAM), dithiothreitol (DTT), guanidine hydrochloride, and $CaCl_2{\cdot}2H_2O$ were obtained from Sigma-Aldrich (USA). Immunoglubulin G-degrading enzyme of *Streptococcus pyogenes* (IdeS) was purchased from RHINO BIO (Suzhou, China). Trypsin for peptide mapping was obtained from Promega (Wisconsin, USA). Ammonium sulfate, sodium dihydrogen phosphate, disodium hydrogen phosphate dihydrate, and *tert*-butyl hydroperoxide (tBHP) were from Sinopharm (Beijing, China). The commercialized Keytruda was purchased from Merck & Co., Inc. (Rahway, N.J., USA). The mAb-A used in this study was a biosimilar of Keytruda, which was manufactured by Shanghai Henlius Biopharmaceutical Co., Ltd. Additionally, mAb-A was utilized as the standard reference in all chromatography, electrophoresis, and mass spectrometry analyses. Each sample was injected once for analysis by chromatography, electrophoresis, mass spectrometry, and peptide mapping.

Chemically Oxidized Sample Preparation. The samples were chemically oxidized using tBHP. The detailed process is as follows: a certain amount of tBHP was added to the mAb-A and Keytruda samples to achieve a final tBHP concentration of 0.25% (v/v). The samples were then incubated in the dark at 2−8 °C for oxidation. The intensity of oxidation can be controlled by adjusting the incubation time (0, 0.5, 4, and 24 h). After oxidation, tBHP was removed through ultrafiltration, and the chemically oxidized samples were stored at −80 °C for further study.

Hydrophobic Interaction Chromatography. The hydrophobicity variant distribution of mAb-A and Keytruda was assessed using HIC analysis. Sepax Proteomix HIC Butyl-NP5 (5 μm, 4.6 × 250 mm) column (DE, USA) was employed on an Agilent 1260 HPLC system (Santa Clara, CA, USA). The mobile phase A consisted of 2 M sodium sulfate in tris-base at pH 7.0, while mobile phase B was tris-base at pH 7.0. The column was operated at a flow rate of 0.5 mL/min at 30 °C. UV detection was performed at a wavelength of 280 nm, and 30 μg of sample was injected.

For antibody analysis, samples were loaded at 55% mobile phase A and 45% mobile phase B. After 3 min, proteins were eluted from the column by increasing mobile phase B from 45% to 100% over 25 min. The column was then washed with 100% mobile phase B for 4 min and equilibrated using the loading condition.

In the fraction collection experiment, a Sepax Proteomix HIC Butyl-NP5 (5 μm, 10 × 250 mm) semipreparative column (DE, USA) was used with a flow rate of 2.0 mL/min and an injection amount of 2 mg. The other conditions were the same as those for the HIC analysis. Fractions corresponding to each peak were manually collected based on UV guidance. The collected samples were subjected to ultrafiltration three times with an excipient solution, followed by HIC analysis to determine the purity of each fraction.

Size Exclusion Chromatography. Size exclusion chromatography (SEC) analysis was performed using an Agilent 1260 system equipped with a TSKgel G3000 column (5 μm, 300 mm × 7.8 mm I.D.) (Japan). The analysis was conducted at room temperature. The mobile phase consisted of 100 mM sodium phosphate supplemented with 0.5% sodium chloride at pH 6.8. A sample of 50 μg was loaded onto the column, and the elution was carried out at a flow rate of 0.5 mL/min for a duration of 30 min.

Cation Exchange Chromatography. CEX was performed using an Agilent 1260 system equipped with a ProPac WCX-10 (4 × 250 mm I.D.) column (Thermo Fisher, Waltham, MA, USA) at a temperature of 35 °C. The UV detector was set at a wavelength of 280 nm. The mobile phase consisted of MES buffer at pH 6.8 for mobile phase A and a mixture of MES buffer at pH 6.8 and 150 mmol/L sodium chloride for mobile phase B. The initial gradient started with 5% mobile phase B and was increased to 35% mobile phase B over a period of 30 min.

Microchip Electrophoresis Sodium Dodecyl Sulfate. In this study, both reduced and nonreduced microchip electrophoresis sodium dodecyl sulfate (ME-SDS) experiments were conducted to analyze molecular size heterogeneity. The experiments were performed using a LabChip GXIITouch system equipped with fluorescence detection and a Protein Express Assay Reagent Kit (PerkinElmer, Waltham, MA, USA). For reduction and alkylation, 1 μM IAM and 4 μM DTT per microgram of protein were used, and the reaction was carried out at 70 °C for 10 min. After the reaction, the test samples were cooled to room temperature, centrifuged, and prepared for ME-SDS analysis.

Reversed-Phase Chromatography and Reduced/IdeS-Digested Molecular Weight Analysis. Reduced and IdeS-digested samples were prepared for RP chromatography and molecular weight analysis. To initiate the reduction process, 0.1 μM DTT per microgram protein was added to the samples, which were then incubated at 37 °C for 10 min. IdeS digestion was performed using 4 units of IdeS per microgram of protein, and the samples were incubated at 37 °C for 1 h. For RP and molecular weight analysis, an Agilent 1290 Infinity LC system coupled with an Agilent 6545XT AdvanceBio Q-Tof mass spectrometer (Santa Clara, CA, USA) was utilized. Separation

https://doi.org/10.1021/acsptsci.4c00296
ACS Pharmacol. Transl. Sci. XXXX, XXX, XXX−XXX

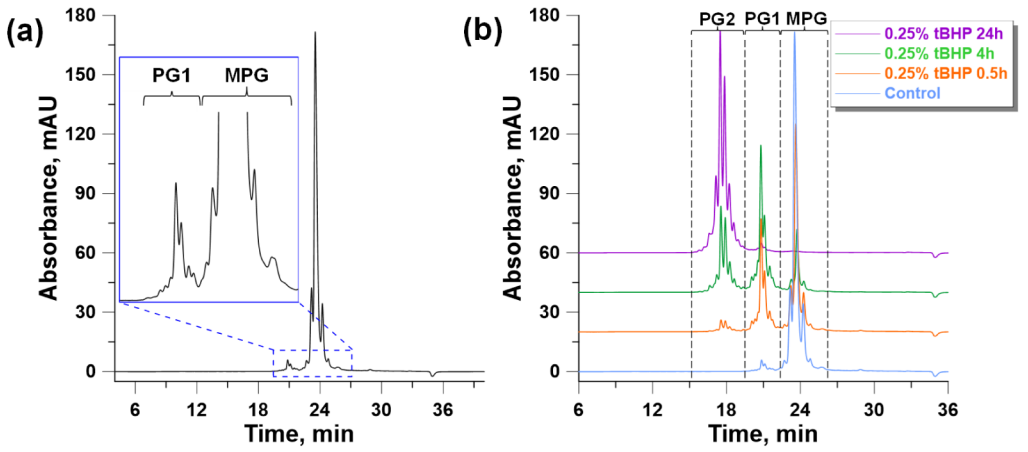

Figure 1. HIC chromatograms of (a) mAb-A and (b) forced oxidized mAb-A (0.25% tBHP for 0, 0.5, 4, and 24 h).

was achieved using a BioResolve RP mAb Polyphenyl column, with a mobile phase consisting of H_2O and ACN containing 0.1% FA. The column temperature was set at 80 °C, and an elution gradient from 5% ACN to 40% was applied over a 15 min period. RP analysis was performed using UV detection at 214 nm, while Q-Tof analysis for molecular weight determination was conducted with a mass range of 400−6000 m/z at a rate of 1 Hz. The obtained mass results were analyzed using Agilent MassHunter BioConfirm software.

Peptide Mapping. The Peptide mapping samples were prepared as follows: First, the samples were denatured by mixing them in a solution containing 6 M guanidine hydrochloride in 50 mM Tris-HCl (pH 8.0). Next, the samples were reduced by adding 10 mM DTT and incubating at 37 °C for 30 min, followed by alkylation with 20 mM iodoacetamide (IAM). After the reduction and alkylation steps, the samples were buffer-exchanged into a solution of 50 mM Tris-HCl and 10 mM $CaCl_2{\cdot}2H_2O$ (pH 7.0) using a NAP-5 column. For further analysis, the samples were incubated with 0.4 μg/μL trypsin. The resulting peptides were then separated using a UPLC C18 column (Waters Acquity UPLC BEH, 2.1 × 150 mm, 1.7 μm) coupled with a Vanquish-QE PLUS LC-MS system (Thermo Fisher, Waltham, MA, USA).

PD-1 Binding Assay. The binding affinity of mAb-A to PD-1 was assessed using an enzyme-linked immunosorbent assay (ELISA). PD-1 antigen was immobilized onto a 96-well plate. Then, serially diluted samples were added for binding, and each sample dilution was prepared in duplicate. Then, a kappa-linked HRP-labeled goat antihuman IgG was used as the secondary antibody. After an enzymatic reaction and chromogenesis, the optical density (OD) of the tested samples was measured by using a microplate reader. Four-parameter logistic regression of raw data was conducted using SoftMax software. The relative binding activity of PD-1 was calculated based on the half-maximum effective concentration (EC_{50}) value obtained from the fitting equation. The collected fraction of entire mAb-A from HIC was used as a reference standard in the PD-1 binding assay.

PD-1/PD-L1 Blockade Bioassay. The inhibitory activity of samples was assessed by using a reporter gene-based PD-1/PD-L1 blockade bioassay. In this assay, CHO-K1 cells that were stably transfected with programmed death-ligand 1 (PD-L1) and aPAC were employed as antigen-presenting cells, while Jurkat cells that were stably transfected with PD-1 and nuclear factor of activated T cells (NFAT) reaction element plasmid were used as effector cells to mimic the PD-1/PD-L1 pathway.

To evaluate the inhibitory effect, the tested samples were serially diluted and specifically bound to PD-1 (each dilution in duplicate), thereby blocking the interaction between PD1 and PD-L1. This blockade resulted in the activation of the NFAT pathway and subsequent expression of the luciferase reporter gene. The expression level of luciferin in the cell supernatant was measured through relative light units (RLU) by a microplate reader. Four-parameter logistic regression via SoftMax software was applied, and the EC_{50} value was calculated to assess the relative inhibition ability of the tested samples. Nonoxidized mAb-A was used as the reference standard in this bioassay.

RESULTS AND DISCUSSION

Development of HIC Method. Keytruda, which serves as the reference medicinal product (RMP) for mAb-A, has been reported to contain oxidation variants in the CDR region.[40] To ensure product quality and similarity to the RMP, it is essential to establish an HIC method for monitoring oxidation variants. The HIC method was developed and optimized, involving the selection of columns, salt types, salt concentration, and pH of the mobile phase. The final optimized HIC chromatogram of mAb-A is shown in Figure 1a. Two distinct peak groups were observed: the main peak group (MPG) eluting at approximately 22−27 min and the prepeak group1 (PG1) eluting at approximately 20−22 min. The earlier elution time of PG1 compared to MPG illustrates a more hydrophilic property, which may be attributed to oxidation or other post-translational modifications.[39,41]

To confirm the presence of oxidation variants, mAb-A was subjected to forced degradation under oxidation conditions and subsequently analyzed using the developed HIC method. Samples with different degrees of oxidation were obtained by incubating mAb-A with 0.25% tBHP at 8 °C for 0 h (control), 0.5 4, and 24 h. As shown in Figure 1b and Table 1, three distinct chromatographic peak groups were observed in the samples with varying degrees of oxidation: prepeak group2 (PG2), PG1, and MPG. Compared to the control sample, the percentage of MPG decreased and the PG1 increased in the sample oxidized for 0.5 h. Additionally, a new peak group, PG2, was observed. The decrease in MPG and the increase in both PG1 and PG2 were more pronounced in the sample oxidized for 4 h. In the sample oxidized for 24 h, the peaks of

https://doi.org/10.1021/acsptsci.4c00296
ACS Pharmacol. Transl. Sci. XXXX, XXX, XXX−XXX

Table 1. Content of PG2, PG1, and MPG for Forced Oxidized MAb-A (0.25% tBHP for 0, 0.5, 4, and 24 h) Using HIC Analysis

oxidation condition	PG2%	PG1%	MPG%
Control	0.0	3.8	96.2
0.5 h	5.2	35.6	59.2
4 h	34.2	48.4	17.4
24 h	94.1	4.2	1.7

MPG and PG1 almost disappeared and the percentage of PG2 significantly increased to 94%. These results suggest that MPG undergoes a progressive conversion to PG1, followed by subsequent conversion to PG2 as the degree of oxidation increases. Thus, it can be speculated that oxidation is the main cause of PG1 and PG2 formation.

Purity Analysis of Forced Degradation Samples. To exclude the possibility that PG1 and PG2 are caused by fragments, aggregates, or charge heterogeneity, SEC, ME-SDS, and CEX methods were also employed to analyze the oxidized samples. As shown in Figure S1 and Table S1, all samples exhibited high purity, and no significant differences in fragments or aggregates were observed. Regarding charge heterogeneity, the ratio of acidic peaks, main peak, and basic peaks remained consistent. These results indicated that the PG1 and PG2 peaks observed in the HIC are not attributed to fragmentation, aggregates, or charge heterogeneity. However, the overlaid CEX chromatogram revealed that retention times of the oxidized samples gradually shifted forward with increasing oxidation. According to the literature, oxidation may affect the antibody structure and surface charge, thereby weakening the binding capacity between the surface charge and the stationary phase.[41] This observation further supports the hypothesis that the formation of PG1 and PG2 groups may be related to oxidation.

RP-HPLC is commonly employed for the analysis of oxidation variants. For instance, Zhang et al. reported that oxidized Fc fragments eluted before the unoxidized fragments on the RP column, and the elution time progressively advanced with an increase in oxidation sites.[42] In this study, oxidized samples with IdeS digestion were analyzed by RP-HPLC. As shown in Figure S2a, the retention time of F(ab')2 gradually shifted forward with increasing oxidation, while the retention time of the Fc peak remained unchanged. Similarly, after DTT reduction, the retention time of the heavy chain (HC) gradually shifted forward with increasing oxidation, while the retention time of LC remains unchanged (as shown in Figure S2b). Met is reported to be the most oxidized amino acid.[43] It is speculated that Met sites on the HC fragment of the fragment of the antigen binding (Fab) region of mAb-A are prone to oxidation, and the number of oxidation sites may increase with prolonged exposure to oxidation conditions. However, it is challenging to separate and monitor oxidation variants of mAb-A solely on the basis of slight changes in peak retention time using RP-HPLC. In conclusion, HIC is the most suitable method for quantifying and monitoring oxidation variants of mAb-A.

Identification of Oxidation Peaks in HIC via Forced Degradation Samples. Molecular weight can provide insights into various post-translational modifications of a molecule, such as oxidation, glycosylation, and N-terminal or C-terminal truncation, among others. In order to specifically identify the oxidation peak in HIC chromatography, molecular weight analysis (LC-MS) was conducted at the subunit level using forced degradation samples. This analysis involved determining the molecular weights of the HC and LC fragments after DTT reduction, as well as molecular weights of the F(ab')2 and Fc/2 fragments after IdeS digestion.

The results of the reduced molecular weight analysis revealed a significant difference in the molecular weight of HC with increasing oxidation, while the molecular weight of LC remained unchanged, as depicted in Figure 2 and Table 2. In the control sample, the predominant molecular weight of HC was primarily 50 707 Da (referred to as H0), which increased to 50 723 Da (referred to as H1) with the progression of oxidation. The increase in the HC molecular

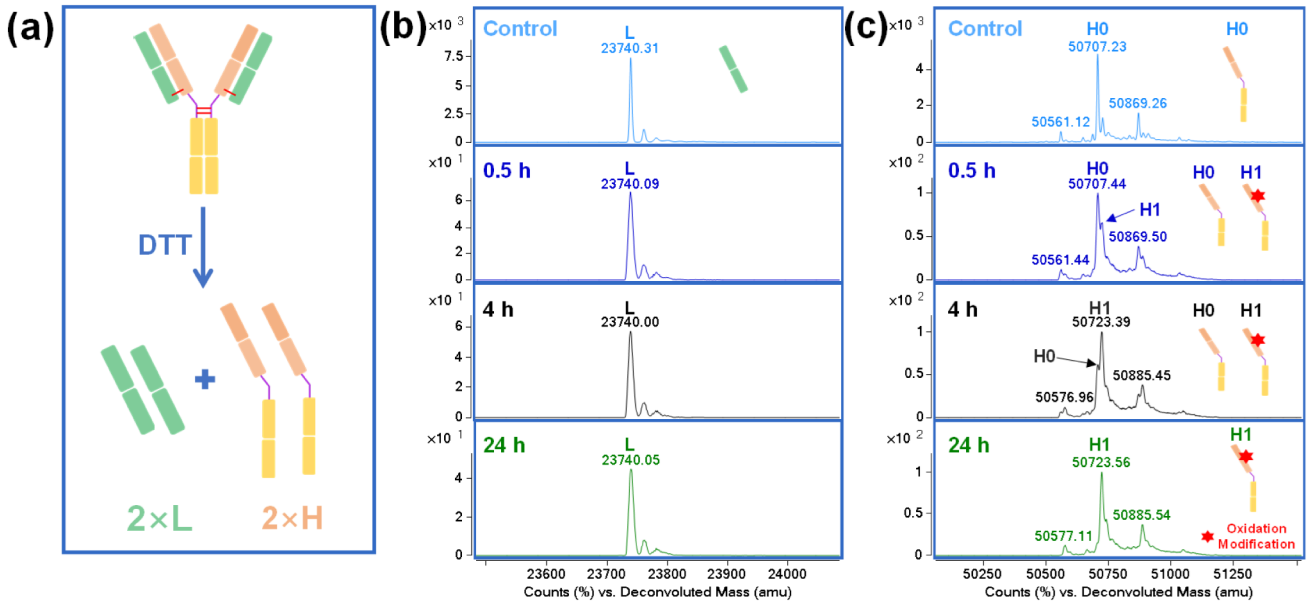

Figure 2. Reduced molecular weight of forced oxidized mAb-A (0.25% tBHP for 0, 0.5, 4, and 24 h). (a) Reduction schematic diagram of mAb-A; (b) light chain deconvolution molecular weight; and (c) heavy chain deconvolution molecular weight.

https://doi.org/10.1021/acsptsci.4c00296
ACS Pharmacol. Transl. Sci. XXXX, XXX, XXX−XXX

Table 2. Reduced and IdeS Digested Molecular Weight for Forced Oxidized mAb-A (0.25% tBHP for 0, 0.5, 4, and 24 h)[a]

oxidation	condition	species	theoretical mass (Da)	observed mass (Da)	mass error (Da)
Reduced	Control	L	23740.67	23740.31	−0.36
		H0	50707.12	50707.23	0.11
		H1	50723.12	ND	/
	0.5 h	L	23740.67	23740.09	−0.58
		H0	50707.12	50707.44	0.32
		H1	50723.12	50723.44	0.32
	4 h	L	23740.67	23740.00	−0.67
		H0	50707.12	50707.80	0.68
		H1	50723.12	50723.39	0.27
	24 h	L	23740.67	23740.05	−0.62
		H0	50707.12	ND	/
		H1	50723.12	50723.56	0.44
IdeS-digested	Control	Fc/2	25216.32	25216.16	−0.16
		F0	98492.97	98491.72	−1.25
		F1	98508.97	ND	/
		F2	98524.97	ND	/
	0.5 h	Fc/2	25216.32	25216.10	−0.22
		F0	98492.97	98492.18	−0.79
		F1	98508.97	98506.13	−2.84
		F2	98524.97	ND	/
	4 h	Fc/2	25216.32	25216.10	−0.22
		F0	98492.97	ND	/
		F1	98508.97	98508.08	−0.89
		F2	98524.97	98522.21	−2.76
	24 h	Fc/2	25216.32	25216.03	−0.29
		F0	98492.97	ND	/
		F1	98508.97	ND	/
		F2	98524.97	98523.55	−1.42

[a]Note: ND, not detected, L = light chain, H = heavy chain, Fc = fragment crystallizable, F = antigen-binding fragment, number in species name refers to the number of oxidative modification sites.

weight indicates that HC underwent oxidation, resulting in a 16 Da increase in molecular weight. In the samples oxidized from 0.5 to 4 h, there was a gradual decrease in the proportion of peak H0 and a corresponding gradual increase in peak H1, suggesting the progressive oxidation of a specific site on HC. In the sample oxidized for 24 h, only the peak H1 was detected, indicating complete oxidation of this specific site. These findings indicate that mAb-A possesses an easily oxidizable site on the HC.

The results of the IdeS-digested molecular weight analysis are listed in Figure S3 and Table 2. The molecular weight of Fc/2 remained constant, while a noticeable difference in the molecular weight of F(ab')2 was observed as oxidation increased. In the control samples, the molecular weight of F(ab') 2 was primarily determined to be 98 492.14 Da. With increasing oxidation, it was found to be 98 508.08 Da (F1) and 98 523.16 Da (F2). This change in subunit molecular weight indicates that sites in F(ab') 2 were easily oxidized, resulting in an increase in molecular weight of 16 and 32 Da, respectively. In the sample oxidized for 0.5 h, the proportion of peak F0 decreased while the corresponding peak F1 gradually increased. This suggests the presence of both unoxidized F(ab') 2 and one oxidized site in F(ab') 2. After a 4 h oxidation duration, only F1 and a significantly increased proportion of F2 were detected. It indicates the presence of both one and two gradually oxidized sites in F(ab') 2. In the sample oxidized for 24 h, only the peak F2 was detected, suggesting that both oxidation-prone sites in F(ab') 2 had been oxidized. These results indicate that mAb-A has two oxidation sites in F(ab') 2 that are prone to oxidation. Additionally, considering the results of reduced molecular weight, there are two symmetrical oxidation-prone sites located on the HC of F(ab') 2, which are referred to as Fd'.

Based on the RP-HPLC and molecular weight analysis, it is evident that amino acid sites in the Fd' fragment of mAb-A have undergone oxidation. Besides, the molecular weight variation observed in the F(ab') 2 fragment aligns with the peak group conversion observed in the HIC analysis. Therefore, it can be inferred that the peak labeled as MPG in the HIC chromatogram corresponds to the unoxidized antibody, while PG1 and PG2 are primarily caused by the hydrophobic heterogeneity resulting from oxidation at one or both HCs in the Fab region of mAb-A.

To pinpoint the exact site of oxidation in mAb-A, forced degradation samples were prepared by treating the antibody with 0.25% tBHP for different durations (0, 0.5, 4, and 24 h). These samples were then analyzed by using reduced peptide mapping (LC-MS/MS) with trypsin digestion. The results, as shown in Table S2, revealed several post-translational modifications in the samples, including N-terminal pyro-glutamylation, amidation at HC: L_{445}, C-terminal lysine truncation, and oxidation at HC: Met_{105}, HC: Met_{252}, and HC: Met_{428} sites. Among these modifications, the oxidation ratio of Met_{105} significantly increased from 3.3% to 94.6% after 24 h of oxidation. The proportions of Met_{252} and Met_{428} oxidation were relatively low and showed a slight increase in the 24 h oxidized sample. No significant changes were observed in other post-translational modifications (PTMs). Therefore, it can be confirmed that the oxidation-prone site of mAb-A is Met_{105} on the HC of Fab, which is consistent with previous speculation. The oxidation of Met_{105} leads to significant hydrophobic differences in the protein, resulting in the appearance of peak groups of PG1 and PG2 in the HIC chromatogram. Besides, the oxidation ratio at the Met_{105} site, which can be calculated from the proportions of PG1 and PG2 in the HIC, is highly consistent with the oxidation ratio detected by PTMs (as shown in Table 3). These findings

Table 3. Comparison of Met_{105} Oxidation Ratio for Forced Oxidized mAb-A (0.25% tBHP for 0, 0.5, 4, and 24 h) between HIC Calculation and PTMs

condition	calculated from HIC (%)	PTMs (%)	difference (%)
Control	1.9	3.3	1.4
0.5 h	23.0	28.2	5.2
4 h	58.4	60.3	1.9
24 h	96.2	94.6	1.6

indicate that PG1 represents the component formed by the oxidation of Met_{105} on one HC, while the PG2 group represents the component formed by the oxidation of Met_{105} on both HCs.

Characterization of Oxidation Variants via Fractionation. To further confirm the formation of each component in HIC, forced oxidation sample of mAb-A (0.25%tBHP for 4 h), which displayed three distinct peak groups in the HIC profile (PG2, PG1, and MPG), was utilized to enrich the components. To separate and collect these components, a semipreparative

https://doi.org/10.1021/acsptsci.4c00296
ACS Pharmacol. Transl. Sci. XXXX, XXX, XXX−XXX

chromatography column was employed. Through this process, we successfully obtained highly pure oxidation variant components. The final purities of PG2, PG1, and MPG components were determined to be 96.2%, 91.5%, and 81.0%, respectively, as shown in Figure 3.

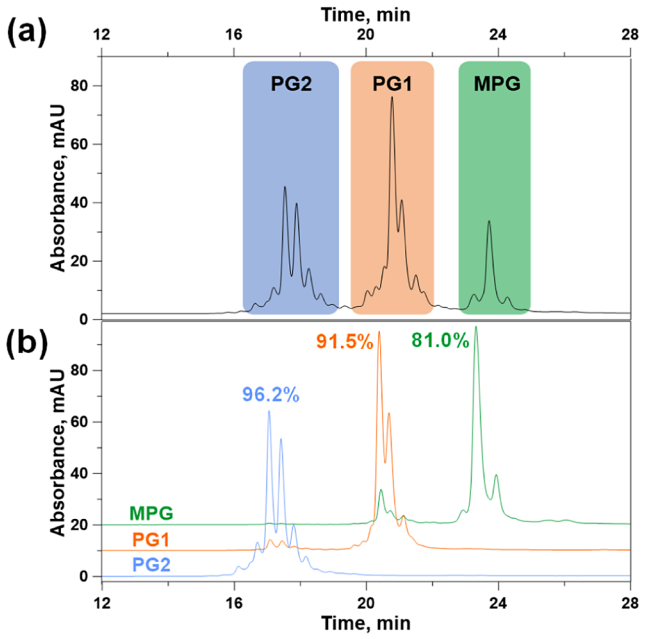

Figure 3. HIC fraction collection of forced oxidized mAb-A by 0.25% tBHP for 4 h. (a) Schematic diagram of HIC fraction collection. (b) Determination of the purity of the collected fractions by HIC method; the purity percentages of each fraction were labeled in the figure with corresponding color.

To characterize PTMs of enriched components, reduced peptide mapping analysis (LC-MS/MS) was performed. The results revealed the presence of several PTMs in MPG, PG1, and PG2 components, including N-terminal pyroglutamylation amidation at HC: L_{445}, C-terminal lysine truncation, as well as oxidation at HC: M_{252} and HC: M_{428}. The modification ratios for these PTMs were found to be similar among the three fractions, as indicated in Table 4. However, it is important to

Table 4. PTMs Results of Collected Fractions

PTMs	MPG%	PG1%	PG2%
Gln→Pyro-Glu (Q_1)	98.2	94.4	91.5
Oxidation (M_{105})	14.1	61.5	96.5
Hydroxylations (K_{124})	5.5	5.2	6.6
Oxidation (M_{252})	3.1	3.4	5.6
Amide (L_{445})	9.4	6.8	5.5
K Loss (K_{447})	98.7	98.0	92.9
Oxidation (M_{428})	1.5	1.5	2.1

note that the oxidation ratio at the HC: M_{105} site differed significantly among the three fractions. The oxidation ratio of the Met_{105} site in the PG2 component was determined to be 96.5%, suggesting that both HCs had undergone nearly complete oxidation at Met_{105}. On the other hand, the oxidation ratio of the Met_{105} in the PG1 component was 61.5%, indicating that at least one of the Met_{105} sites had undergone oxidation. Therefore, it can be concluded that the PG1 component primarily consists of oxidation at one HC's Met_{105} site, while the PG2 component is predominantly formed by oxidation at both HC's Met_{105} sites. This conclusion aligns with the initial identification of oxidation variants in the HIC analysis using forced degradation samples.

Structure and Function Relationship Study of Oxidation Variants. The impact of Met oxidation on the structure and function of antibodies has been extensively studied, particularly in the Fc region. Studies have shown that when the oxidation ratio of Met_{257} reaches 80%, significant changes occur in the protein structure, leading to a decrease in FcRn binding and CDC activity to less than 20%.[44] In the case of mAb-A, the HC: Met_{105} oxidation occurs in the CDR region. However, there is limited literature available on the impact of oxidation in the CDR region on the biological function of the antibody. Hence, we conducted a biological assay using the Met_{105} oxidized components to evaluate their effect on the antibody's biological function.

To assess the Fab-related activities, we performed PD-1 binding and PD-1/PD-L1 cell-based blockade assays. As shown in Table 5, the PD-1 binding activity of all three

Table 5. PD-1 Binding Activity and PD-1/PD-L1 Blockade Activity of the Collected Fractions

components	PD-1 binding activity	PD-1/PD-L1 blockade activity
MPG	109%	94%
PG1	113%	30%
PG2	119%	9%

fractions ranged from 109% to 119%, which falls within the acceptable range of 70−130%. This indicates that Met_{105} oxidation has no significant effect on the binding activity of the antibody. The PD-1/PD-L1 blockade activity, which is mediated through the Fab domain and initiates a cascade of signaling pathways leading to T-cell activation and tumor cell targeting and killing,[45] was 94% for the MPG fraction. However, as depicted in Figure S4, the PG1 and PG2 components showed a significant reduction in PD-1/PD-L1 blockade activity with values of 30% and 9%, respectively. These results revealed that Met_{105} oxidation in the CDR region significantly impairs the antibody's ability to block PD-1/PDL1 interactions. It is hypothesized that oxidation may lead to modifications in higher-order structures, resulting in biologically less active products compared to their native counterpart.[3]

Validation of the HIC Method. The research findings indicate that oxidation at Met_{105} is the primary cause of the prepeak groups observed in the HIC chromatogram of mAb-A. This oxidation has a significant impact on the PD-1/PD-L1 blockade function. To quantitatively analyze the oxidation, the developed method needs to be validated according to ICH guideline Q2(R1). The specificity of the HIC method was confirmed, showing no interfering peaks. The method also demonstrated excellent linearity within the concentration range of 0.5−2.0 mg/mL. Accuracy was satisfactory, with recovery values ranging from 98.8% to 116.5%. The LOD and LOQ shown in Table S3 were determined to be 0.01% and 0.07%, respectively. Precision was satisfactory, with RSD values of 0.6% (MPG) and 13.2% (PG1) for repeatability and 0.5% (MPG) and 10.9% (PG1) for reproducibility. Sample stability was confirmed for up to 48 h at 8 °C. Overall, the established HIC method offers good resolution, robustness, precision, and accuracy for assessing and controlling the quality of mAb-A.

https://doi.org/10.1021/acsptsci.4c00296
ACS Pharmacol. Transl. Sci. XXXX, XXX, XXX−XXX

Application of HIC in Analytical Similarity Study. The established HIC method in this study allows for the quantitative analysis of oxidation variants in mAb-A, with a particular focus on monitoring the oxidation of Met_{105} in the CDR region. This method is stability indicative and can be utilized for process control, release test, and stability studies, as well as other purposes aimed at monitoring the content of oxidation. Furthermore, as mAb-A is a biosimilar to Keytruda, the establishment of an HIC method can aid in investigating the similarity in the quality attributes of oxidation.

To assess the similarity between mAb-A and Keytruda, one lot of each was selected for HIC analysis after tBHP incubation for different time intervals (0, 0.5, 4, and 24 h) to compare their degradation rates in terms of oxidation. The results, as depicted in Figure 4 and Table S4, demonstrate complete

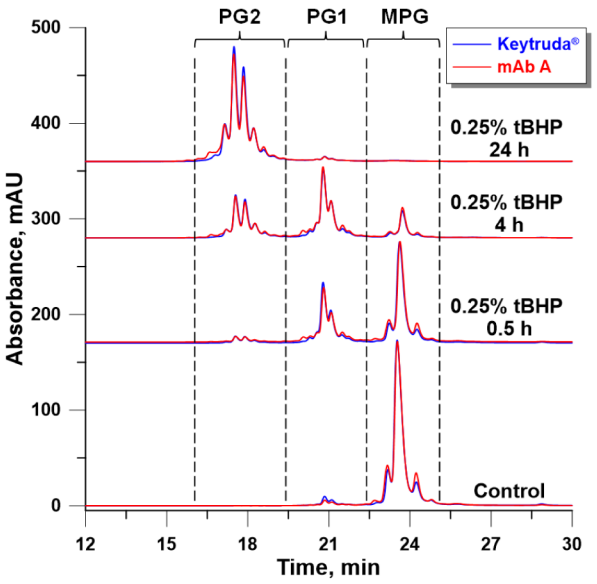

Figure 4. Similarity comparison of forced oxidized Keytruda and mAb-A (0.25% tBHP for 0, 0.5, 4, and 24 h).

overlap in the HIC profiles of mAb-A and Keytruda. Additionally, the proportions of peak areas shared the same variation as the oxidation duration increased, indicating that mAb-A and its originator share the same degradation products and degradation rate.

CONCLUSIONS

In this study, we utilized the HIC method to analyze samples with varying degrees of oxidation in order to investigate the oxidation patterns of mAb-A. Our results revealed that mAb-A is susceptible to oxidation, as indicated by the increased proportion of PG1 and the appearance of a new PG2 group in the HIC chromatogram with increasing oxidation levels. We conducted enrichment and characterization of the oxidation components. Our analysis supported the conclusion that the PG1 component corresponds to oxidation at the HC: Met_{105} site in the CDR region on one heavy chain of mAb-A, while the PG2 component is associated with oxidation at the HC: Met_{105} site in the CDR region on two heavy chains of mAb-A. Futhermore, we investigated the biological functions of the oxidation components. Our findings demonstrated that Met_{105} oxidation in the CDR region does not significantly affect PD-1 binding activity but does significantly reduce PD-1/PD-L1 cell-based blockade activity.

Additionally, we have successfully established a stable and reliable HIC method for the quantitative analysis of Met_{105} oxidation in the CDR region, which is a critical quality attribute for mAb-A. This method will support the product release and stability studies. We evaluated the analytical similarity between mAb-A and the RMP Keytruda in terms of the quality attribute of oxidation. By elucidating the oxidation patterns and investigating the biological consequences of oxidized mAb-A, this study has provided valuable insights that can serve as a blueprint for the adoption of similar analytical approaches across the antibody industry.

ASSOCIATED CONTENT

Supporting Information

The Supporting Information is available free of charge at https://pubs.acs.org/doi/10.1021/acsptsci.4c00296.

Summary of SEC, ME-SDS, and CEX results for forced oxidized samples (Table S1); PTMs% results for forced oxidized samples (Table S2); validation results for the HIC method (Table S3); HIC analysis results comparison of forced oxidation samples between mAb-A and Keytruda (Table S4); CEX, ME-SDS, SEC, and RP profiles for forced oxidized mAb-A (Figures S1 and S2); IdeS-digested MW analysis of forced oxidation samples (Figure S3); and PD-1/PD-L1 cell-based blockade activity (Figure S4) (PDF)

AUTHOR INFORMATION

Corresponding Authors

Lei Zhang − *Analytical Science Development, Henlius Biologics Co., Ltd, Shanghai 201616, China;* orcid.org/0000-0002-7353-4826; Email: Lei_Zhang@henlius.com

Zhongli Zhang − *Analytical Science Development, Henlius Biologics Co., Ltd, Shanghai 201616, China;* orcid.org/0000-0001-6248-191X; Email: Zhongli_Zhang@henlius.com

Authors

Liu Tang − *Analytical Science Development, Henlius Biologics Co., Ltd, Shanghai 201616, China*

Huiliang Geng − *Analytical Science Development, Henlius Biologics Co., Ltd, Shanghai 201616, China*

Xinyi Wang − *Analytical Science Development, Henlius Biologics Co., Ltd, Shanghai 201616, China*

Mengdan Fei − *Analytical Science Development, Henlius Biologics Co., Ltd, Shanghai 201616, China*

Boyuan Yang − *Analytical Science Development, Henlius Biologics Co., Ltd, Shanghai 201616, China*

Haijie Sun − *Analytical Science Development, Henlius Biologics Co., Ltd, Shanghai 201616, China*

Complete contact information is available at: https://pubs.acs.org/10.1021/acsptsci.4c00296

Author Contributions

‡L.T. and H.G. contributed equally to this work. L.T. performed writing—original draft and acquisition. H.G. performed acquisition and analysis. L.Z. performed writing—review and editing and conceptualization. X.W. performed acquisition. M.F. reviewed the manuscript. B.Y. performed

https://doi.org/10.1021/acsptsci.4c00296
ACS Pharmacol. Transl. Sci. XXXX, XXX, XXX−XXX

acquisition and data processing. H.S. performed the experiments. Z.Z. provided the resources.

Notes

The authors declare no competing financial interest.

■ ACKNOWLEDGMENTS

There is no funding associated with the work featured in this article.

■ REFERENCES

(1) Folzer, E.; Diepold, K.; Bomans, K.; Finkler, C.; Schmidt, R.; Bulau, P.; Huwyler, J.; Mahler, H. C.; Koulov, A. V. *J. Pharm. Sci.* **2015**, *104* (9), 2824−2831.
(2) Gupta, S.; Jiskoot, W.; Schöneich, C.; Rathore, A. S. *J. Pharm. Sci.* **2022**, *111* (4), 903−918.
(3) Torosantucci, R.; Schöneich, C.; Jiskoot, W. *Pharm. Res.* **2014**, *31* (3), 541−553.
(4) Ji, J. A.; Zhang, B.; Cheng, W.; Wang, Y. J. *J. Pharm. Sci.* **2009**, *98* (12), 4485−4500.
(5) Valley, C. C.; Cembran, A.; Perlmutter, J. D.; Lewis, A. K.; Labello, N. P.; Gao, J.; Sachs, J. N. *J. Biol. Chem.* **2012**, *287* (42), 34979−34991.
(6) Gao, X.; Ji, J. A.; Veeravalli, K.; John Wang, Y.; Zhang, T.; McGreevy, W.; Zheng, K.; Kelley, R. F.; Laird, M. W.; Liu, J.; Cromwell, M.; et al. Effect of individual Fc methionine oxidation on FcRn binding: Met252 oxidation impairs FcRn binding more profoundly than Met428 oxidation. *J. Pharm. Sci.* **2015**, *104* (2), 368−377.
(7) Cymer, F.; Thomann, M.; Wegele, H.; Avenal, C.; Schlothauer, T.; Gygax, D.; Beck, H. *Biologicals* **2017**, *50*, 125−128.
(8) Wang, W.; Vlasak, J.; Li, Y.; Pristatsky, P.; Fang, Y.; Pittman, T.; Roman, J.; Wang, Y.; Prueksaritanont, T.; Ionescu, R. *Mol. Immunol.* **2011**, *48* (6−7), 860−866.
(9) Stracke, J.; Emrich, T.; Rueger, P.; Schlothauer, T.; Kling, L.; Knaupp, A.; Hertenberger, H.; Wolfert, A.; Spick, C.; Lau, W.; et al. *MAbs* **2014**, *6* (5), 1229−1242.
(10) Boyd, D.; Kaschak, T.; Yan, B. *J. Chromatogr B Analyt Technol. Biomed Life Sci.* **2011**, *879* (13−14), 955−960.
(11) Dashivets, T.; Stracke, J.; Dengl, S.; Knaupp, A.; Pollmann, J.; Buchner, J.; Schlothauer, T. *MAbs* **2016**, *8* (8), 1525−1535.
(12) Illyés, E. *Int. J. Biochem. Res. Rev.* **2014**, *4*, 367−385.
(13) Wecksler, A. T.; Yin, J.; Lee Tao, P.; Kabakoff, B.; Sreedhara, A.; Deperalta, G. *Mol. Pharmaceutics* **2018**, *15* (4), 1598−1606.
(14) Joubert, M. K.; Luo, Q.; Nashed-Samuel, Y.; Wypych, J.; Narhi, L. O. *J. Biol. Chem.* **2011**, *286* (28), 25118−25133.
(15) Luo, Q.; Joubert, M. K.; Stevenson, R.; Ketchem, R. R.; Narhi, L. O.; Wypych, J. *J. Biol. Chem.* **2011**, *286* (28), 25134−25144.
(16) Wong, C.; Strachan-Mills, C.; Burman, S. *J. Chromatogr. A* **2012**, *1270*, 153−161.
(17) Pavon, J. A.; Li, X.; Chico, S.; Kishnani, U.; Soundararajan, S.; Cheung, J.; Li, H.; Richardson, D.; Shameem, M.; Yang, X. *J. Chromatogr. A* **2016**, *1431*, 154−165.
(18) Du, Y.; Walsh, A.; Ehrick, R.; Xu, W.; May, K.; Liu, H. *MAbs* **2012**, *4* (5), 578−585.
(19) Liu, S.; Madren, S.; Feng, P.; Sosic, Z. *J. Pharm. Biomed. Anal.* **2020**, *185*, 113217.
(20) Yuan, J. J.; Gao, D.; Hu, F.; Shi, Y.; Wu, Z. H.; Hu, C. Q.; Huang, X. D.; Fang, W. J.; Zhang, H. T.; Wang, H. B. *J. Chromatogr B Analyt Technol. Biomed Life Sci.* **2021**, *1162*, 122485.
(21) Hensel, M.; Steurer, R.; Fichtl, J.; Elger, C.; Wedekind, F.; Petzold, A.; Schlothauer, T.; Molhoj, M.; Reusch, D.; Bulau, P. *PLoS One* **2011**, *6* (3), No. e17708.
(22) Xu, C.; Khanal, S.; Pierson, N. A.; Quiroz, J.; Kochert, B.; Yang, X.; Wylie, D.; Strulson, C. A. *Anal. Bioanal. Chem.* **2022**, *414* (29−30), 8317−8330.
(23) Kwok, T.; Zhou, M.; Schaefer, A.; Bo, T.; Li, V.; Huang, T.; Chen, T. *Anal. Methods* **2023**, *15* (4), 411−418.
(24) Wei, Z.; Feng, J.; Lin, H. Y.; Mullapudi, S.; Bishop, E.; Tous, G. I.; Casas-Finet, J.; Hakki, F.; Strouse, R.; Schenerman, M. A. *Anal. Chem.* **2007**, *79* (7), 2797−2805.
(25) Qi, P.; Volkin, D. B.; Zhao, H.; Nedved, M. L.; Hughes, R.; Bass, R.; Yi, S. C.; Panek, M. E.; Wang, D.; Dalmonte, P.; et al. *J. Pharm. Sci.* **2009**, *98* (9), 3117−3130.
(26) Lu, Y.; Williamson, B.; Gillespie, R. *Curr. Pharm. Biotechnol.* **2009**, *10* (4), 427−433.
(27) Rodriguez-Aller, M.; Guillarme, D.; Beck, A.; Fekete, S. *J. Pharm. Biomed. Anal.* **2016**, *118*, 393−403.
(28) Cusumano, A.; Guillarme, D.; Beck, A.; Fekete, S. *J. Pharm. Biomed. Anal* **2016**, *121*, 161−173.
(29) Eakin, C. M.; Miller, A.; Kerr, J.; Kung, J.; Wallace, A. *Front. Pharmacol.* **2014**, *5*, 87.
(30) Haverick, M.; Mengisen, S.; Shameem, M.; Ambrogelly, A. *MAbs* **2014**, *6* (4), 852−858.
(31) Fekete, S.; Veuthey, J. L.; Beck, A.; Guillarme, D. *J. Pharm. Biomed. Anal.* **2016**, *130*, 3−18.
(32) King, C.; Patel, R.; Ponniah, G.; Nowak, C.; Neill, A.; Gu, Z.; Liu, H. *J. Chromatogr B Analyt Technol. Biomed Life Sci.* **2018**, *1085*, 96−103.
(33) Wei, B.; Han, G.; Tang, J.; Sandoval, W.; Zhang, Y. T. *Anal. Chem.* **2019**, *91* (24), 15360−15364.
(34) Cao, M.; De Mel, N.; Wang, J.; Parthemore, C.; Jiao, Y.; Chen, W.; Lin, S.; Liu, D.; Kilby, G.; Chen, X. *J. Pharm. Sci.* **2022**, *111* (2), 335−344.
(35) Mohamed, H. E.; Al-Ghobashy, M. A.; Abbas, S. S.; Boltia, S. A. *J. Pharm. Biomed. Anal.* **2023**, *228*, 115249.
(36) Fleming, R. *Methods Mol. Biol.* **2020**, *2078*, 147−161.
(37) Manzke, O.; Tesch, H.; Diehl, V.; Bohlen, H. *J. Immunol. Methods* **1997**, *208* (1), 65−73.
(38) Chen, T.; Han, J.; Guo, G.; Wang, Q.; Wang, Y.; Li, Y. *Protein Expr. Purif.* **2019**, *164*, 105457.
(39) Valliere-Douglass, J.; Wallace, A.; Balland, A. Separation of populations of antibody variants by fine tuning of hydrophobic-interaction chromatography operating conditions. *J. Chromatogr. A* **2008**, *1214*, 81−89.
(40) Sundaramurthi, P.; Chadwick, S.; Narasimhan, C. *J. Oncol. Pharm. Pract.* **2020**, *26* (3), 641−646.
(41) Ruppen, I.; Beydon, M. E.; Solís, C.; Sacristán, D.; Vandenheede, I.; Ortiz, A.; Sandra, K.; Adhikary, L. *Biologicals* **2022**, *77*, 1−15.
(42) Zhang, B.; Jeong, J.; Burgess, B.; Jazayri, M.; Tang, Y.; Taylor Zhang, Y. *J. Chromatogr B Analyt Technol. Biomed Life Sci.* **2016**, *1032*, 172−181.
(43) Kim, G.; Weiss, S. J.; Levine, R. L. *Biochim. Biophys. Acta* **2014**, *1840* (2), 901−905.
(44) Mo, J.; Yan, Q.; So, C. K.; Soden, T.; Lewis, M. J.; Hu, P. *Anal. Chem.* **2016**, *88* (19), 9495−9502.
(45) Zitvogel, L.; Kroemer, G. *Oncoimmunology* **2012**, *1* (8), 1223−1225.

https://doi.org/10.1021/acsptsci.4c00296
ACS Pharmacol. Transl. Sci. XXXX, XXX, XXX−XXX